J Mater Sci (2011) 46:5925–5930
DOI 10.1007/s10853-011-5546-0

Fabrication of superhydrophobic surfaces on aluminum substrates using $NaNO_3$ electrolytes

**Wenji Xu · Jinlong Song · Jing Sun ·
Qingle Dou · Xujuan Fan**

Received: 19 January 2011 / Accepted: 6 April 2011 / Published online: 13 April 2011

Abstract A superhydrophobic surface with a water contact angle of 166.0° and a tilting angle of 1.5° was fabricated on an aluminum substrate by electrochemical machining using neutral $NaNO_3$ electrolytes, followed by fluorination. The fabrication process is based on the fact that the grain boundaries and dislocations on aluminum are anodic dissolved before the grain itself by an applied electric field. Using scanning electron microscopy to analyze surface morphology, micrometer scale caves, and protrusions were found on the surface, with numerous nanometer mastoids contained in the protrusions. These binary micro-nano rough structures, which are similar to the micro-structures of a lotus leaf surface, play an important role in achieving superhydrophobicity. The effects of processing time, processing current, and electrolyte concentration on superhydrophobicity were also examined. The results show that electrochemical machining does not require rigid processing parameters, uses a simple device, and is highly efficient and environmental friendly. The optimum processing conditions are a processing time of 60 min, a processing current of 250 mA, and an electrolyte of 0.15 mol/L.

Introduction

Wettability is one of the important properties of solid surfaces which is commonly measured using the contact angle. For the hydrophilic, superhydrophilic, hydrophobic, and superhydrophobic surfaces, the contact angle is less than 90°, 5°, larger than 90°, and 150°, respectively. In nature, the superhydrophobic phenomenon is evident everywhere. Lotus leaves, rice leaves, and other plant leaves have a self-cleaning effect [1]. Water striders can stand effortlessly and move quickly on water [2]. Butterfly wings do not get wet in the rain [3]. The fabrication and application of superhydrophobic surfaces on metallic substrates have attracted substantial interest among researchers due to these surfaces' self-cleaning [4–7], drag reduction [8–10], corrosion resistance [11, 12], and anti-icing effects [13–18].

To date, many artificial superhydrophobic surfaces have been fabricated successfully on certain metallic substrates such as Al, Cu, Zn, Ni, Au, Fe, and Ti. Ohkubo et al. [19] fabricated superhydrophobic and oleophobic surfaces on aluminum via sandblasting using grained Al_2O_3, followed by anodization in the electrolyte of phosphoric acid, and subsequent treatment with heptadecafluoro-1,1,2,2-tetrahydrodecyltrimethoxysilane (HDFS). Shirtcliffe et al. [20] used electrodeposition and mask lithography to deposit rough copper pillars on smooth copper base surfaces in order to obtain a superhydrophobic surface with a contact angle of 165° after coating with a fluorocarbon hydrophobic layer. Qian and Shen [21] reported on the fabrication of superhydrophobic surfaces on aluminum, copper, and zinc with dislocation etchant and fluoroalkylsilane. They found that the treated surfaces exhibit a water contact angle larger than 150°, and a tilting angle less than 10°. Larmour et al. [22] coated zinc on silver and copper on gold by electroless galvanic deposition, and fabricated superhydrophobic surfaces with a contact angle of 173° ± 1° and a tilting angle of 0.64° ± 0.04° after modification with HDFT. Liu et al. [11] obtained a superhydrophobic surface on copper with a contact angle of 155° through the one-step solution immersion method

---

W. Xu (✉) · J. Song · J. Sun · Q. Dou · X. Fan
School of Mechanical Engineering, Dalian University of Technology, Dalian 116024, People's Republic of China
e-mail: wenjixu@dlut.edu.cn

without any surface modification. Tieme et al. [23] used siloxane rubber and epoxy resin as templates to replicate the microstructure of a lotus leaf on pure aluminum, and achieved a superhydrophobic surface with a contact angle of 161° following chemical modification with hexadecyltrimethoxysilane. These previous studies have advanced knowledge on the fabrication of superhydrophobic surfaces on metallic substrates, but the following key issues remain to be addressed. (1) Anodization and chemical etching need to use a corrosive solution such as acid and alkali. (2) Electrodeposition requires complex equipment, and (3) the materials needed in electroless galvanic deposition are also costly. (4) Further, the one-step solution immersion method requires a longer processing time or the use of a strong alkali. (5) Finally, the template prepared by the template method cannot be used repeatedly.

The current paper reports on a new approach to fabricate a superhydrophobic surface on aluminum substrates by applying neutral $NaNO_3$ electrolytes and an applied electric field, which can induce the grain boundaries and dislocations to dissolve prior to the grain itself in order to form binary micro-nano rough structures. A superhydrophobic surface with a contact angle of 166.0° and a tilting angle of 1.5° is obtained after modification with fluoroalkylsilane. This preparation method is advantageous as it does not require rigid processing parameters, uses a simple device, and is highly efficient and environmental friendly.

Experiment

Materials

An aluminum plate with purity $\geq 99\%$ was obtained from Dalian Aluminum Material Manufacturer, China. A copper plate was obtained from Tianjin Kermel Chemical Reagent Co., China. Fluoroalkylsilane (tridecafluoroctyltriethoxysilane (FAS), $C_8F_{13}H_4Si(OCH_2CH_3)_3$) was obtained from Degussa Co., Germany, and the other experiment drugs used were of analytical grade (Tianjin Kermel Chemical Reagent Co., China).

Fabrication of the superhydrophobic surfaces

Through addition of 1 g FAS into 99 g anhydrous ethanol at room temperature in a beaker, followed by stirring with a magnetic stirrer at a speed of 100 r/min for 2.5 h, 1.0 wt% fluoroalkylsilane–ethanol solution was prepared. A $NaNO_3$ aqueous solution of 0.15 mol/L was obtained by adding a certain amount of $NaNO_3$ into 1 L of deionized water. A $30 \times 30 \times 2$ mm aluminum plate was polished mechanically using 1500# metallographic abrasive paper, and cleaned ultrasonically in sequence with alcohol and deionized water. After drying, the anodic aluminum plate and cathodic copper plate with the same size as the anode were parallel positioned with a distance of 30 mm. Then the aluminum plate was electrochemically machined in the 0.15 mol/L $NaNO_3$ aqueous solution at a current of 250 mA for 60–210 min at room temperature. After machining, the specimens were ultrasonically rinsed with deionized water for 5 min and dried. Modification of the aluminum specimens with low surface energy material was performed by dip-coating them in 1.0 wt% fluoroalkylsilane–ethanol solution for 3 h at room temperature, followed by heat-treated at 100 °C for 20 min.

Characterization

The microstructure of the superhydrophobic surface was observed by scanning electron microscopy (SEM, JSM-6360LV, Japan). The water contact angles were measured by an optical contact angle meter (Krüss, DSA100, Germany) at ambient temperature. Water droplets of 5 μL were dropped carefully onto the surfaces, and the average value of five measurements at different positions of the specimens was used as the final contact angle. The tilting angle is defined as the angle at which the water drop begins to roll off the gradually inclined surface.

Results and discussion

Analysis of the binary micro-nano structures on aluminum

Microstructures and wettability on the aluminum surface

Figure 1 shows the SEM images of the aluminum surfaces treated in 0.15 mol/L $NaNO_3$ aqueous solution at 250 mA for 60 min, as well as image of the water droplets on the as-prepared aluminum surface. Figure 1a shows the image with 200× magnification. Many round pits with diameters of 30–50 μm and fractal rough structures are distributed on the aluminum surface, with some of the round pits closely linked to one another. Figure 1b shows the image of the fractal rough structures with 2,000× magnification. An alveolate structure which consists of connected anomalistic micrometer scale caves and protrusions is fabricated. The inset of Fig. 1b is a higher resolution image with 9,000× magnification; it shows that numerous nanometer mastoids are contained in the micrometer scale protrusions. Figure 1c shows the round pits in Fig. 1a with 5,000× magnification, indicating that nanometer grains exist on the wall of the round pits. Therefore, there are binary micro-nano rough structures similar to the microstructures of the

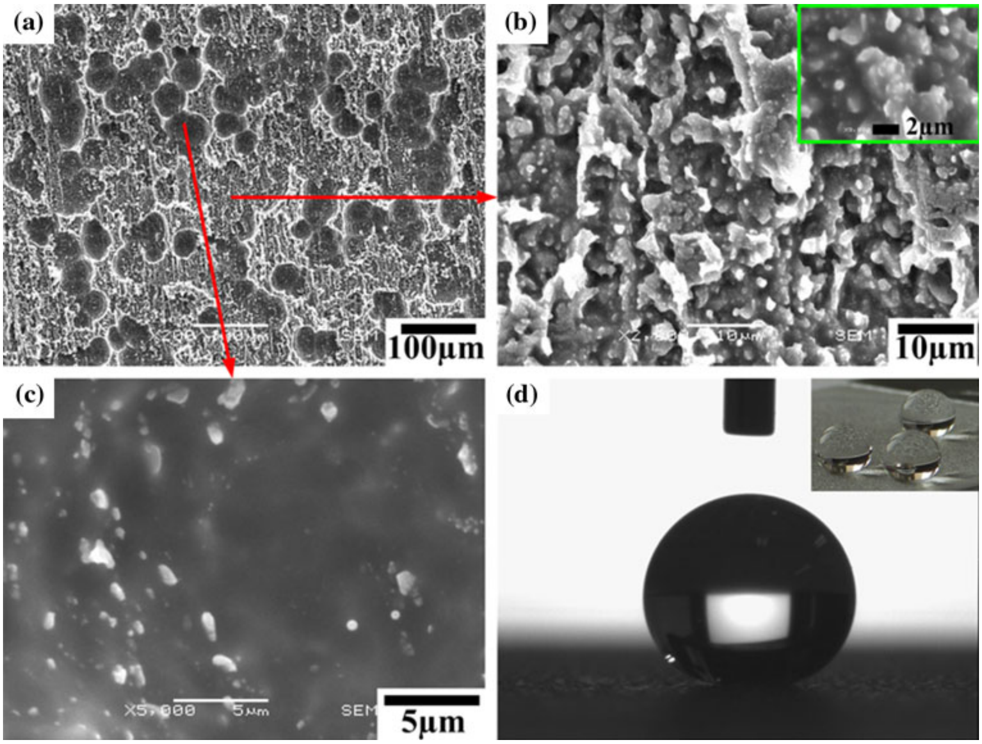

Fig. 1 SEM images of the aluminum surfaces after processing and optical image of the droplets on the as-prepared surfaces with **a** ×200 magnification; **b** ×2,000 magnification image of the fractal rough structures. The *inset* is obtained at a higher resolution with *bar* = 2 μm; **c** ×5,000 magnification image of the round pits; **d** water droplets with a volume of 5 μL

lotus leaf surface in fractal rough structures and round pits. These rough structures play an important role in achieving superhydrophobicity. After electrochemical machining, the aluminum surfaces also exhibit superhydrophilic properties before fluorination, and water droplets spread on the surface completely with a contact angle of about 0°. This phenomenon conforms to Wenzel's theory [24] that roughness enhances the hydrophilicity of hydrophilic surfaces.

As shown in Fig. 1d, a 5 μL water droplet exhibits a typical spherical shape with a contact angle of 166.0° and a tilting angle of 1.5° on the superhydrophobic surface. This superhydrophobic behavior can be explained theoretically in terms of the Cassie–Baxter model [25], which is described as follows:

$$\cos\theta_c = f_1\cos\theta - f_2$$

where θ_c (166.0°) and θ (108°) represents the contact angles on the rough and smooth aluminum surfaces, respectively, which are both modified by fluoroalkylsilane. f_1 and f_2 are the fractional interfacial areas of the binary micro-nano rough structures and of the trapped air in the voids among the rough structures, respectively ($f_1 + f_2 = 1$). From this equation, we can deduce that an increase in the fraction of air (f_2) can increase the contact angle of the rough surface (θ_c). According to the equation, f_1 and f_2 are estimated to be 0.043 and 0.957, respectively. Therefore, when a water droplet is placed on the superhydrophobic surface on aluminum, only about 4.3% serves as the contact area of the water droplet and the solid surface, and the remaining 95.7% serves as the contact area of the water droplet and air.

Analysis of the binary micro-nano rough structures obtained

There are numerous grain boundaries and dislocations in aluminum crystal [26, 27]; the former has a general scale running from several microns to tens of microns, whereas the latter runs in nanometer scale. Grain boundaries are prone to be anodic dissolved and to undergo priority erosion due to their special composition and arrangement. Similarly, dislocations, especially in special sites such as outcrops, are also conducive to electrochemical reaction and the fabrication of caves on the surface due to their relatively high energy. Therefore, micrometer scale caves and protrusions, as well as nanometer mastoids in the protrusions and grains in Fig. 1c, are assumed to result from the preferential dissolution of grain boundaries and dislocations by an applied electric field.

The electrolyte used in this study is the neutral $NaNO_3$ aqueous solution, which is a non-linear electrolyte having a low current efficiency when the current density is small. The applied current density is about 27.8 mA/cm^2, and the current efficiency is relatively low, so oxygen evolution reaction occurs with the dissolution of the anode, generating oxygen bubbles. When the bubble volume increases, the buoyancy increases. When the buoyancy is beyond the adhesion to the substrate, the bubbles detach from the surface of the substrate and carry off corrosion products, but they fill the fresh electrolyte. These result in a large quantitative corrosion and eventually form round pits with a smooth wall.

Effect of processing time on hydrophobicity

Figure 2 and Table 1 show the variation in water contact angle and tilting angle with the processing time. The contact angle increases significantly with an increase in processing time from 15 to 60 min. The contact angle of the surface after 15 min of processing and fluoroalkylsilane modification reaches 144.36°, because a certain roughness is obtained after electrochemical machining, thus enhancing the surface hydrophobicity as shown in Fig. 3a. However, due to the uneven roughness and non-corroded areas, the tilting angle becomes as large as 20°. When the processing time extends to 30 min, the surface roughness becomes uniform, the contact angle increases to 158.49°, and the tilting angle decreases to 4°. When the processing time goes beyond 60 min, the contact and the tilting angles remain stable. Figure 3b shows the SEM image of the aluminum surface treated for 210 min. Round pits with diameters of 100 μm are distributed evenly and are linked closely. The partially enlarged image also shows micro-nano caves and mastoids instead of nanometer grains, which are similar to the round pits in Fig. 1b.

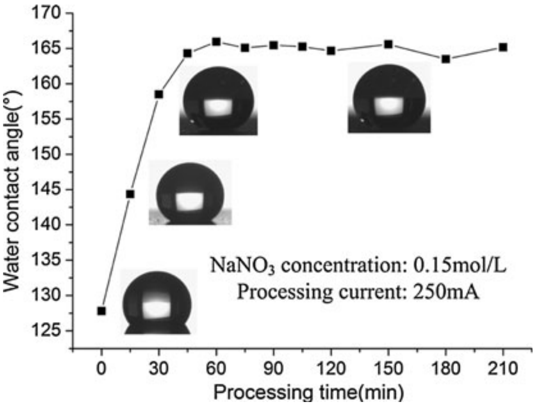

Fig. 2 Relationship between processing time and the contact angle on the superhydrophobic surfaces of aluminum

Table 1 Relationship between processing time and the tilting angle

Processing time (min)	Tilting angle (°)
0	None
15	20
30	4
45	3
60	1.5
75–210	1

Effect of processing current on hydrophobicity

Figure 4 and Table 2 show the variation in water contact angle and tilting angle with the processing current. The contact angle increases significantly with an increase in the processing current from 50 to 250 mA, with the tilting angle decreasing correspondingly. As shown in Fig. 5a, the contact angle of the aluminum surface treated at 50 mA and modified with fluoroalkylsilane only reached 132.42°, whereas the tilting angle was so large that a 5 μL water droplet still adhered to the surface when the specimens were turned over 180°. This is because $NaNO_3$ is a non-linear and passive electrolyte. Further, the processing current of 50 mA results in a very low current efficiency. Therefore, a passive film is generated on aluminum to prevent the workpiece from being corroded, except in the area where oxygen evolution reaction takes place and the substrate contacts the fresh electrolyte. Therefore, due to the large interval of round pits and non-corroded areas, there are insufficient rough structures, leading to a low contact angle and large tilting angle.

When the processing current goes beyond 250 mA, the contact angle decreases significantly, with a corresponding increase in the tilting angle. Figure 5 shows the SEM image of the aluminum surface treated at 450 mA with uniform and shallow round pits but unnoticeable microstructures. This is due to the increase in removal amount with an increase in current efficiency, which in turn increases with a rise in processing current. However, the state with a contact angle of 158.58° and a tilting angle of 10° is caused by the nanometer grains that can be seen from the inset of Fig. 5. This phenomenon conforms to Jiang's [28] theory that a high contact angle is induced by nanostructures, and a low tilting angle is induced by micro-nano structures.

Effect of $NaNO_3$ concentration on hydrophobicity

Figure 6 and Table 3 show the variation in water contact angle and tilting angle with $NaNO_3$ concentration. Hydrophobicity is affected slightly by the $NaNO_3$ concentration in the range of 0.05–0.65 mol/L. It remains constant at a contact angle above 160° and a titling angle less than 3°.

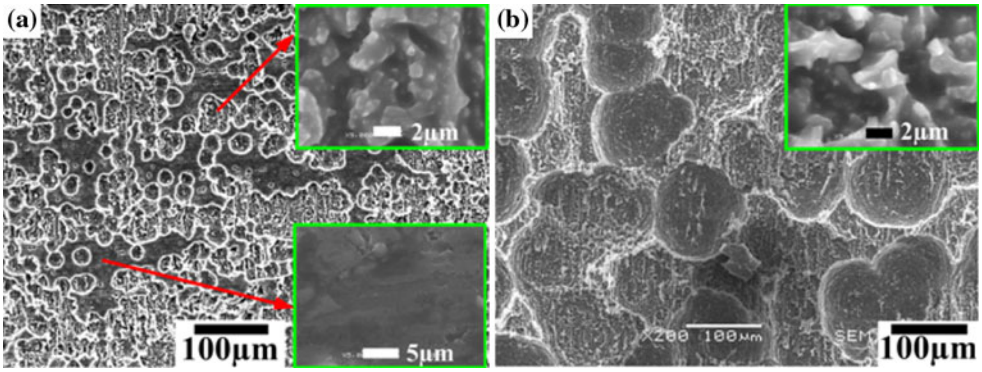

Fig. 3 SEM images of the aluminum surfaces at different processing times: **a** 15 min, **b** 210 min

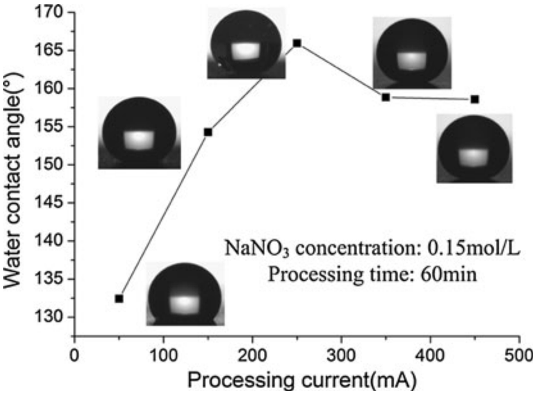

Fig. 4 Relationship between processing current and the contact angle on the superhydrophobic surfaces of aluminum

Table 2 Relationship between processing current and the tilting angle

Processing current (mA)	Tilting angle (°)
50	None
150	7
250	1.5
350	2
450	10

Conclusion

(1) Superhydrophobic surfaces with a water contact angle of 166.0° and a tilting angle of 1.5° were fabricated on aluminum substrates by electrochemical machining using neutral $NaNO_3$ electrolytes, followed by fluorination. Compared with traditional methods, the method proposed in the current paper does not require a strong acid and a strong base. It is also advantageous in that it does not require rigid processing parameters, uses a simple device, and is highly efficient and environment friendly.

(2) Processing conditions such as electrolyte concentration, processing current, and time were investigated to determine their effect on the surface superhydrophobicity. The optimum processing conditions were a processing time of 60 min, a processing current of 250 mA, and a $NaNO_3$ electrolyte of 0.15 mol/L.

(3) Superhydrophobicity on an aluminum substrate is generated by micro-nano cavies and protrusions which are assumed to be caused by the preferential dissolution of grain boundaries and dislocations by an applied electric field. After electrochemical machining, the aluminum surfaces exhibit superhydrophilic properties before fluorination with a contact angle of about 0°.

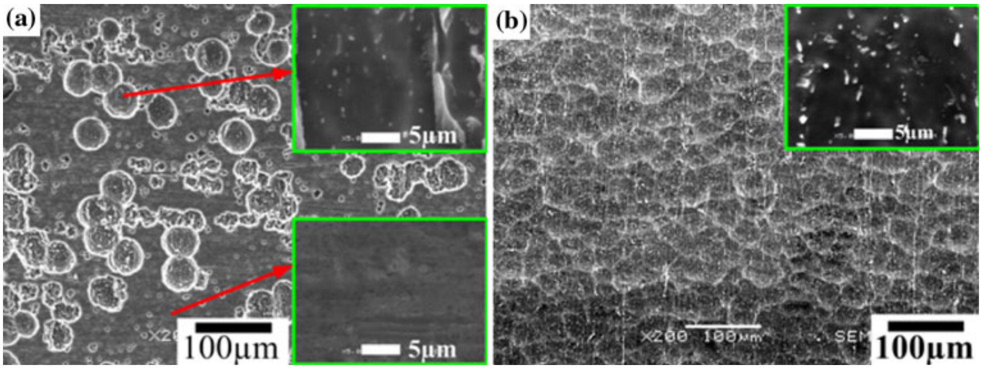

Fig. 5 SEM images of the aluminum surfaces at different processing currents: **a** 50 mA, **b** 450 mA

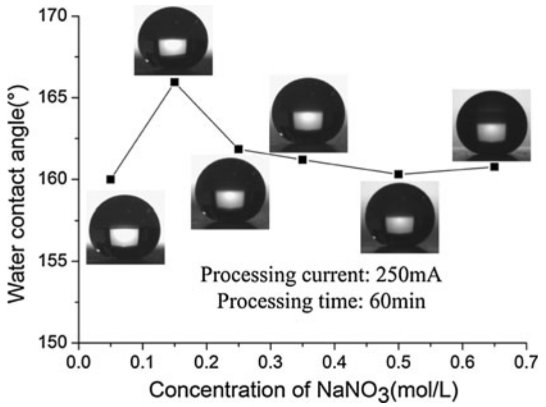

Fig. 6 Relationship between $NaNO_3$ concentration and the contact angle on the superhydrophobic surfaces of aluminum

Table 3 Relationship between $NaNO_3$ concentration and the tilting angle

$NaNO_3$ concentration (mol/L)	Tilting angle (°)
0.05	1.5
0.15	1.5
0.25	1.5
0.35	2
0.5	3
0.65	3

(4) The superhydrophobic behavior is explained theoretically in terms of the Cassie–Baxter model. Only about 4.3% serves as the contact area of the water droplet and the solid surface.

Acknowledgement The authors thank for the financial support from the National Science Foundation of China (No. 90923022).

References

1. Barthlott W, Neinhuis C (1997) Planta 202:1
2. Gao XF, Jiang L (2004) Nature 432:36
3. Wang H, Tang LM, Wu XM, Dai WT, Qiu YP (2007) Appl Surf Sci 253:8818
4. Wagner T, Neinhuis C, Barthlott W (1996) Acta Zool 77:213
5. Furstner R, Barthlott W, Neinhuis C, Walzel P (2005) Langmuir 21:956
6. Lee HJ (2009) J Mater Sci 44:4645. doi:10.1007/s10853-009-3711-5
7. Hayn RA, Owens JR, Boyer SA (2011) J Mater Sci 46:2503. doi:10.1007/s10853-010-5100-5
8. Mchale G, Shirtcliffe NJ, Evans CR, Newton MI (2009) Appl Phys Lett 94:064104
9. Watanabe K, Yanuar, Udagawa H (1999) J Fluid Mech 381:225
10. Shi F, Niu J, Liu JL, Liu F, Wang ZQ, Feng XQ, Zhang X (2007) Adv Mater 19:2257
11. Liu T, Yin YS, Chen SG, Chang XT, Cheng S (2007) Electrochim Acta 52:3709
12. Yin YS, Liu T, Chen SG, Liu T, Cheng S (2008) Appl Surf Sci 255:2978
13. Kulinich SA, Farzaneh M (2009) Appl Surf Sci 255:8153
14. Yin L, Xia Q, Xue J, Yang SQ, Wang QJ, Chen QM (2010) Appl Surf Sci 256:6764
15. Cao LL, Jones AK, Sikka VK, Wu JZ, Gao D (2009) Langmuir 25:12444
16. Tourkine P, Merrer ML, Quere D (2009) Langmuir 25:7214
17. Suzuki S, Nakajima A, Yoshida N, Sakai M, Hashimoto A, Kameshima Y, Okada Y (2007) Chem Phys Lett 445:37
18. Wang H, Tang LM, Wu XM, Dai WT, Qiu YP (2007) Appl Surf Sci 253:8818
19. Ohkubo YJ, Tsuji I, Onishi S (2010) J Mater Sci 45:4963. doi:10.1007/s10853-010-4362-2
20. Shirtcliffe NJ, Mchale G, Newton MI, Chabrol G, Perry DC (2004) Adv Mater 16:1929
21. Qian BT, Shen ZQ (2005) Langmuir 21:9007
22. Larmour IA, Bell SEJ, Saunders GC (2007) Angew Chem 119:1740
23. Thieme M, Frenzel R, Schmidt S, Simon F, Hennig A, Worch H, Lunkwitz K, Scharnweber D (2001) Adv Eng Mater 3:691
24. Wenzel RN (1936) Ind Eng Chem 28:988
25. Cassie ABD, Baxter S (1996) Trans Faraday Soc 40:546
26. Henderson B (1972) Defects in crystalline solids. Edward Arnold Ltd, London
27. Hull D, Bacon DJ (2001) Introduction to dislocations. Butterworth-Heinemann, Oxford
28. Feng L, Li SH, Li YS, Li HJ, Zhang LJ, Zhai J, Song YL, Liu BQ, Jiang L, Zhu DB (2002) Adv Mater 14:1857